

Development of Polymer Nanocomposites for Rapid Prototyping Process

M.S.Wahab, K.W.Dalgarno, R.F.Cochrane, S.Hassan *Member, IAENG*

Abstract-This paper presents initial development of polymer nanocomposites (PNC) material for rapid manufacturing (RM) application. PNC materials containing a polyamide (PA) and nano particles (5wt%) were produced by solution blending with the aim to improve the mechanical properties. Commercial polyamide 6 (PA6) was dissolved in formic acid (HCO₂H) together with two different types of nano particle materials: yttrium stabilised zirconia (YSZ) and Hectorite clay (Benton 166) and spray-dried to create powder, creating powder with particle sizes in the range of 10-40 µm. The materials were processed on a CO₂ selective laser sintering (SLS) experimental machine. Mechanical properties of the PNCs were evaluated and the results were compared with the unfilled base polymer.

Index Terms-Rapid Manufacturing (RM), Layer Manufacturing (LM), Selective Laser Sintering (SLS), Polymer nanocomposite (PNC)

I. INTRODUCTION

Several technologies known as layer manufacturing processes have been developed over the past 10-15 years to shorten the product development cycle [1]. The techniques are all based on the principle of creating three-dimensional components directly from computer aided design (CAD) in two-dimensional profiles on layer-by-layer process without using moulds or tools as used in conventional manufacturing techniques [2-4]. To date, the layer manufacturing processes have been used to produce physical components for various purposes: patterns for prototyping, fit/assembly components and also functional models [5-6]. In fact, some of the layer manufacturing processes are already being used in rapid manufacturing to produce finished components (or at least near finished) for small volume production. Boeing and NASA are examples of industries using layer manufacturing processes for direct fabrication of aircraft and aerospace components [7].

Manuscript received February 10, 2009. This work was supported in part by University Tun Hussein Onn Malaysia under university scholarship for postgraduate study.

M. S. Wahab and S. Hassan are with the Manufacturing and Industrial Engineering Department, Faculty of Mechanical and Manufacturing Technology, Universiti Tun Hussein Onn Malaysia, 86400 Parit Raja, Batu Pahat, Johor, Malaysia (phone: +(607)4537752; fax: +(607)4536080; e-mail: saidin@uthm.edu.my).

K. W. Dalgarno was with School of Mechanical Engineering, University of Leeds, LS29JT. He is now with the School of Mechanical and System Engineering, Newcastle University (e-mail: kenny.dalgarno@newcastle.ac.uk).

R. F. Cochrane is with the School of Process, Environmental and Materials Engineering, Leeds University (e-mail: R.F.Cochrane@leeds.ac.uk).

There is a variety of layer manufacturing techniques available today, for example stereolithography (SLA), selective laser sintering (SLS), fused deposition modelling (FDM), three-dimensional printing (3DP), and others [8]. For the application of rapid manufacturing, SLS has an advantage to produce parts from a relatively wide range of commercially available materials, including polymer (nylon, also glass-filled or with other fillers, and polystyrene) [9].

The production costs using SLS also appear to be significantly less than for other layer manufacturing techniques, particularly when compared with SLA and FDM process [10]. This makes SLS have a great future potential for rapid manufacturing application for production of end-used products and is therefore the process that is chosen in this investigation.

Selective laser sintering was developed by Carl Deckard for his master's thesis at the University of Texas and was patented in 1989 [11]. The technique, shown schematically in Figure 1, uses a laser beam to selectively fuse powdered materials into a solid object.

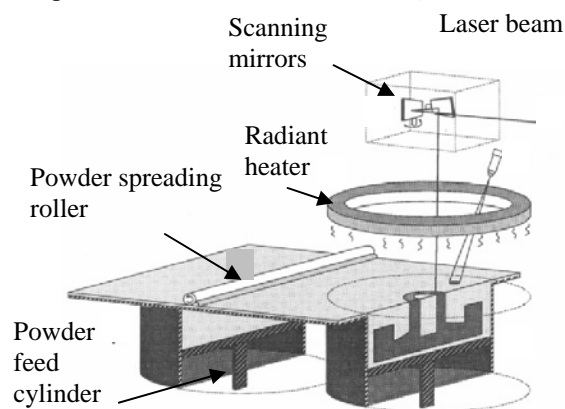


Fig. 1 Schematic diagram of selective laser sintering [12]

Parts are built upon a platform which sits just below the surface in a bin of the heat-fusible powder. A laser traces the pattern of the first layer, sintering it together. The platform is lowered by the height of the next layer and powder is reapplied. This process continues until the part is complete. Excess powder in each layer helps to support the part during the build.

In the area of rapid manufacturing, mechanical properties of produced part become critically important where the stiffness, strength and surface finish must be sufficient to meet in-service loading and operation requirements [13]. In addition, the mechanical properties must be comparable to those produced using traditional manufacturing routes to make the layer manufacturing-based process competitive.

Many efforts are under way to develop high-performance rapid manufacturing materials for engineering applications, including enhanced mechanical properties [14-16], transparency film and flammability [17] by using polymer nanocomposites (PNC) materials as an example.

PNCs are based on controlling the microstructure of materials by incorporating nanometer-size material as second-phase dispersions into polymer matrixes [18]. PNCs have emerged as materials which can show significantly enhanced mechanical properties over those of the base polymer through the addition of relatively small amounts of nano-scale additives. Improvements in strength and modulus of 40-70% have been reported to have arisen as a result of addition of 2-5wt% of nano clay [19], for example. Despite their attractiveness, the full potential of PNCs has still not been realised for layer manufacturing applications, particularly for SLS. Although some progress has already been reported elsewhere concerning the fabrication, microstructure and properties of PNC, significant gaps in knowledge still exist. None is devoted to polyamide-6 (PA6) nanocomposites, processed using the SLS process.

The overall work in this research is therefore to examine whether or not using PNCs as a raw material in SLS can overcome to some degree of the limitations of the currently available material, through reinforcement of nano-size particles to improve the mechanical properties.

II. EXPERIMENT PROCEDURE

A. Materials

Different type of nano additive materials has been used to reinforce with Polyamide 6 (PA6). Yttrium stabilized zirconia (YSZ) is a ceramic base material and was received from AMR Technologies. It contain components of zirconium oxide >94% and yttrium oxide at 5.4%. The key properties of the YSZ are high fracture toughness, high hardness and thermal resistance [20]. Modified organoclay BENTON166 was received from Elementies Specialist (UK). The BENTON166 is an alkylaryl ammonium hectorite clay material and it has been developed as an additive for most polymer system. The key properties are for high mechanical strength and improve flame retardant characteristic [21].

The PA6, a semi-crystalline, white engineering thermoplastic with an average size of 15-20µm was purchased from Goodfellow (UK) [22].

B. Preparation of polymer nanocomposites

The preparation procedure is shown schematically in Figure 2 and it is aim to prepare the material with a good dispersion of the additive in the polymer material. The good dispersion is importance to gain a benefit from the present of nano particles.

The nano particles as well as the PA6 powder were dissolved in polar organic solvent formic acid (HCO₂H) on separate container and stirred at room temperature for 3hrs, followed by ultrasonic bath for 20 minutes. Formic

acid proved to be sufficient solvent for nylon in particular of PA6, as no heat needed to be added to the system in order to induce dissolution. Then the dispersed nano particles was added into the PA6 solution with composition of 5wt% and continue stirred for another 4hrs to ensure uniform mixing of polymer and nano particles is achieved. A spray dryer Labplant SD05 as shown in Figure 3 is used to produce powder from the solution.

The spray drying process involves the atomization of a liquid feedstock into a spray of droplets and contacting the droplets with hot air in a drying chamber [18]. For evaluating the effect of the solution concentration, the spray drying was performed with various concentration levels of the PA6 solution from 100g/litre, 50g/litre and 30g/litre. Higher concentrations did not spray in the form of droplets, but lower concentrations produced too small particles and consumed a lot of solvent. Then the collected powder continues for further drying process in an oven at 70°C for another 4hrs to remove the remaining solvent in the powder. Then the process was continued with a ball milled for two hrs to segregate any agglomerated powder and sieved them with sieve size of 200 micron and finish with 70 micron.

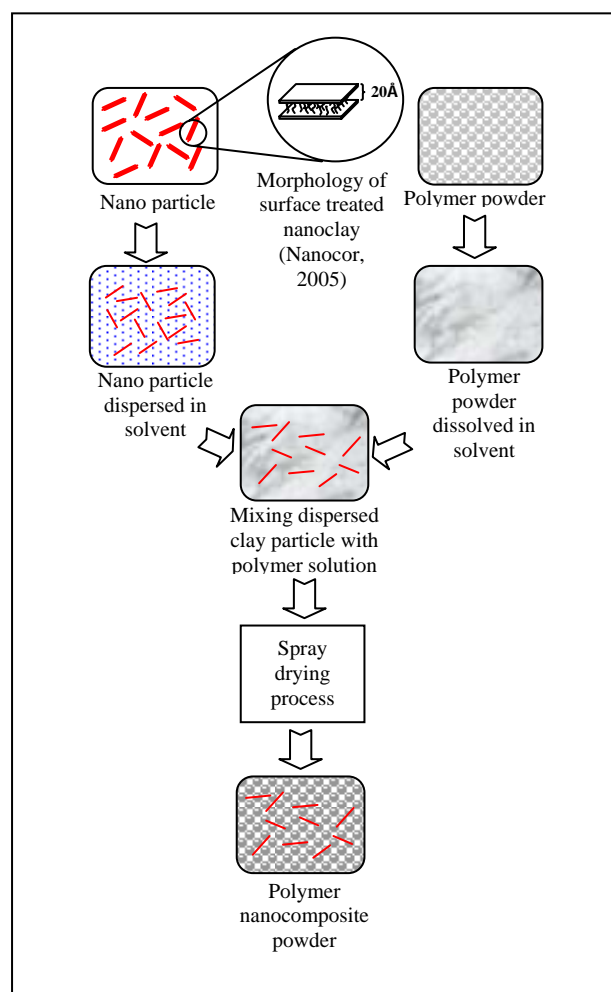


Fig. 2 Schematic representation of preparation procedure for PNC, consisting of nano additive particle and PA6 by using a solution method



Fig. 3 SD-05 spray dryer machine used in production of powder

C. Characterisation

Differential scanning calorimetry (DSC) was performed on a Perking-Elmer DSC 7 under nitrogen purge at a heating and cooling rate of 10°C/min. 10mg of samples were heated from room temperature 30°C to 250°C. Measurement of tensile strength was carried out using Dartec machine with 5kN load cell and the cross head movement of 1 mm/min. Specimens were fabricated using SLS experimental machine based on ASTM D638 type V standard [23]. Each test was executed with five individual specimens and results for ultimate tensile strength were evaluated. TEM and SEM were used to observe the dispersion of nano additive and analyzed the fracture surface morphology of the processed material.

D. SLS processing

CO₂ SLS experimental machine with the build volume (X,Y,Z) is 75mm x 75mm x 100mm has been used to fabricate the test specimen as shown in Figure 4. The machine was constructed at the University of Leeds [24] equipped with CO₂ laser with a wavelength of 10.6µm and maximum output power of 250W with a 0.6 mm beam diameter.



Fig. 4 CO₂ SLS experimental machine used to fabricate test specimen

The test specimens have been fabricated using process parameters setting of 10 Watt laser power, 500 mm/s scanning speed, 0.6 mm scan size, 0.1 mm scan spacing and 0.1 mm layer thickness.

III. RESULTS AND DISCUSSION

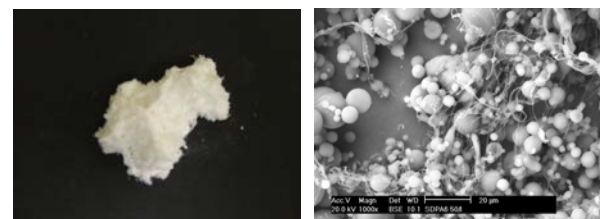
A. Effect of solution concentration level

The morphology structures of the spray-dried powders are shown in Figure 5. SEM images showed that at higher concentration level of 100g/litre, Figure 5(a), a lot of fibres were produced with fewer powder particles observed. Most of the fibres were spread in the drying chamber and caused trapped powders from going to the collecting bottle.

By reducing the concentration to 50g/litre, Figure 5(b), the amount of particles produced was increased with fewer fibres, but most of the particles were found attached together with the fibres and were difficult to separate even by sieving. The concentration was further reduced to 30g/litre, Figure 5(c), and the result showed more powders were received and almost no fibres were produced. This phenomenon is well known as being related to the viscosity, which varies with the concentration of the solution. Fong [25] described this as the effect of viscosity and surface tension. At a low concentration, the viscosity of the solution is low, while the surface tension is relatively high. Therefore, the solution jet could not maintain its own shape at the end of the tip due to high surface tension and gave a small drop which would form powder. On the other hand, at high concentrations, the viscosity of the solution is also high, so the drop was produced in continuous form which would give fibres as well as powder.



(a) Concentration of 100g/litre



(b) Concentration of 50g/litre



(c) Concentration of 30g/litre

Fig. 5 Photographic images and SEM images of sample powder from spray dryer process prepared with different concentration levels

The powders produced from the spray dryer were spherical in shape with various sizes estimated in a range of 5-40 μm . Some of the small particles were attached to the bigger particles. This is probably due to the effect of the adsorption force of the small particles on the surface of the bigger particles. The optimum inlet and outlet temperatures were estimated to be 180 $^{\circ}\text{C}$ and 110 $^{\circ}\text{C}$, the rate of air drying was 0.47 mm^3/min and the atomising pressure was 1.5 kgf/cm^3 .

The particle size distribution of the spray-dried powder was measured using laser diffraction technique, Malvern Mastersizer E. The measured mean size was 30 μm , with some particles at below 1 μm , as shown in Figure 6.

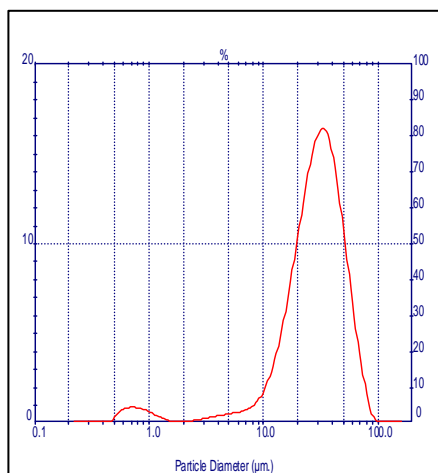


Fig. 6 Particle size measurement

B. Dispersion of nano additive in PA6 matrix

PA6/YSZ nanocomposite

Figure 7 shows SEM images of PA6/YSZ powder produced from spray drier process. Some small white contrast particles were observed on PA6/YSZ and uniformly distributed on the powders. This was believed to be the coarse or agglomerated particles present in the YSZ and this was confirmed by TEM and EDX analysis, shown in Figure 8. This was though due to the effect from the changes in viscosity in the combined PA6 solution and nano additive suspension. Increasing viscosity could reduce the mobility of the nano particles and could promote agglomeration within the nano particles.

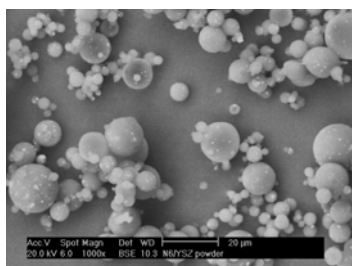


Fig. 7 SEM images of PNC powders produced from spray dryer process

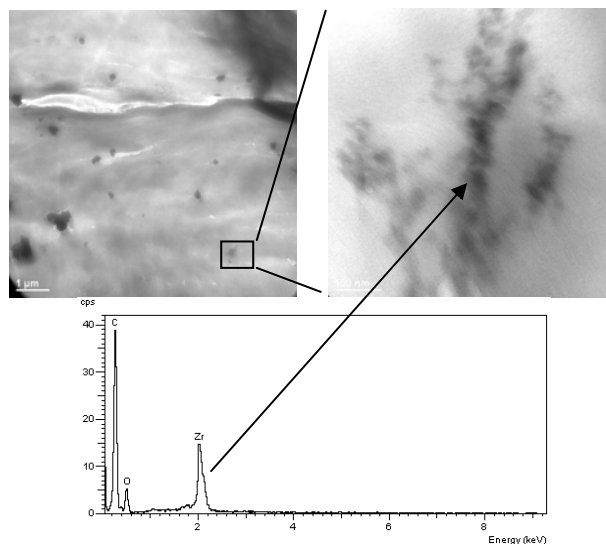


Fig. 8 TEM micrograph images of the SLS processed PA6/YSZ nanocomposites and EDX analysis for white contrast on the image.

PA6/B166 nanocomposite

Figures 9 and 10 shows SEM and TEM images of the PA6/B166 nanocomposite powder. It can be seen that the dispersion of the clays was randomly across the PA6 matrix, suggesting good dispersion was achieved. Some sticking particles were still observed, meaning that the particles were having strong interaction between the layers, which requires more shear process to break them.

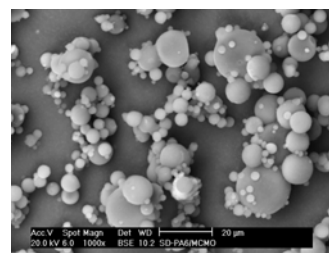


Fig. 9 SEM image of the PA6/clay nanocomposite.

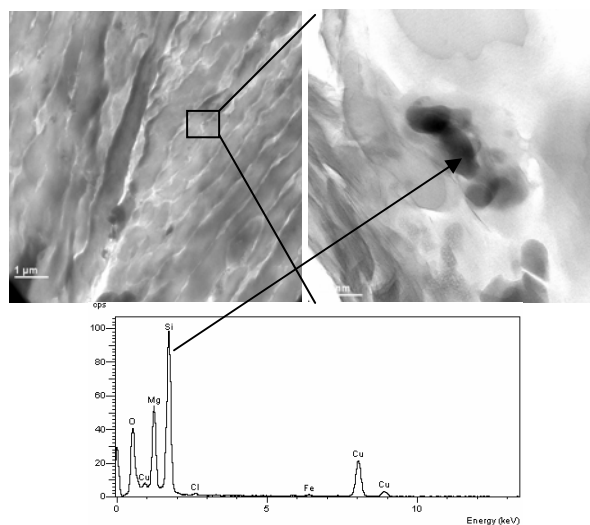
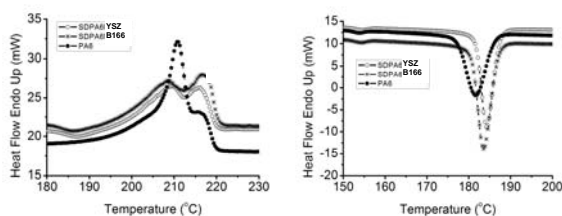


Fig. 10 TEM micrograph images of the spray dried PA6/B166 and EDX analysis on the clay particle.

C. Thermal properties

Figure 11 shows DSC results for PNC's and the unfilled PA6, highlighted at the peaks area during heating and cooling process. During heating, the PA6 and the composites show endotherms with two melting peaks. According to Sessa [26], this double melting phenomenon ascribed due to bimodal crystallite distribution is common to nylons like PA6 and is a characteristic of melts crystallised at a heating rate of 10°C/min. Further, the appearance of dual melting peaks in both the neat PA6 and PNC proves that this is not due to the presence of additives generated in the system under study. The higher temperature peak represents the melting point (T_m) of the α -form crystal of PA6, and the lower temperature peak resulted from imperfect crystals. Only one exothermic peak temperature (T_c) was observed for each cooling curve between 179°C and 183°C. The addition of clays raised T_c by about 2-4°C, and T_c did not change very much with different clays materials.



(a) Heating (b) Cooling

Fig. 11 Melting and cooling process

D. Mechanical properties

Figure 12 shows the results for the average tensile properties of the PNCs and the unfilled PA6. The results show a reduction of tensile strength for spray dried PA6 material as compared to the as received PA6. Similar results were also found for the PA6/YSZ and PA6/B166 nanocomposite materials where the tensile strength was lower than that of the as received unfilled PA6 material, but it's slightly higher than that of the spray dried PA6. Spray dried PA6/YSZ and PA6/B166 nanocomposite materials with 5wt% additives were found to have strengths 50-60% higher on average than that of spray dried PA6 without reinforcement. This suggests that the reinforcement of Hectorite clays in PA6 has improved its properties. However, it clear that the spray drying process has an adverse effect on the base mechanical properties.

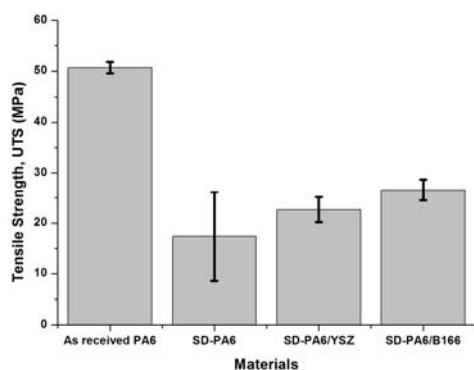
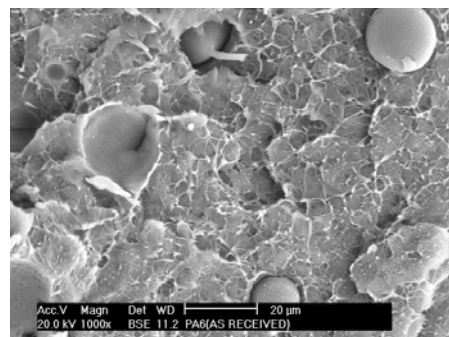


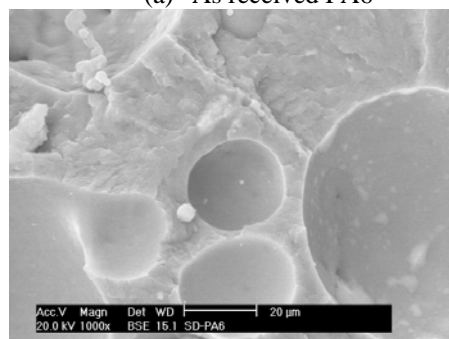
Fig. 12 Tensile strength result for the PNCs and the unfilled PA6

E. Microscopy of tensile fracture surface

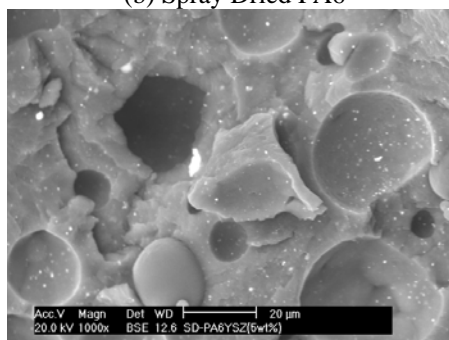
Figure 13 shows SEM images of tensile fracture surfaces of the sintered specimens for the spray dried material. The sintered materials contain voids which would act to reduce density and strength. Most of the voids for the spray dried material are spherical in shape and bigger than those in the as received PA6.



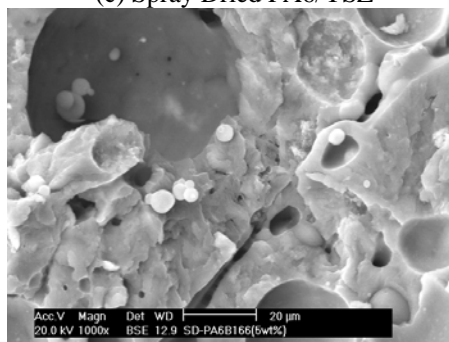
(a) As received PA6



(b) Spray Dried PA6



(c) Spray Dried PA6/YSZ



(d) Spray Dried PA6/B166

Fig. 13 SEM images of tensile fracture surface of as received PA6 and PNC (5wt%)

This suggests that the cause could be from the trapped gases generated from residual solvent from the

spray drying being driven off during laser sintering. Further research work to provide information and understanding about the creation of voids in the SLS specimen for the spray dried material.

IV. CONCLUSION

The following conclusions were drawn from this study:

1. PA6/YSZ and PA6/B166 nanocomposite materials have been successfully prepared by solution blending, followed by spray drying.
2. The TEM observation on SLS processed PNC materials have shown that good dispersion of the YSZ and B166 clay in PA6 matrix were achieved.
3. SLS fabrication of near-full dense samples for the PNC material was possible.
4. The spray drying process was found to reduce the tensile strength of the PA6 material.

REFERENCES

1. Debasish, D., Fritz, B. P., David, R., Lee, W. *Layer manufacturing: Current status and Future Trends*. ASME, 1, 2001, pg. 60-69.
2. Kruth, J. P., Leu, M. C., & Nakagawa, T. Progress in additive manufacturing and rapid prototyping. *CIRP Annals - Manufacturing Technology*, 47(2), 1998, pg. 525-540.
3. Pham, D. T., Learning factory rapid prototyping. Available from www.me.psu.edu/lamancusa/rapidpro/primer/chapter2.htm. [Accessed 26/12/04].
4. Levy, G. N., & Schindel, R. *Overview of layer manufacturing technologies, opportunities, options and applications for rapid tooling*. Proceedings of the Institution of Mechanical Engineers, Part B: Journal of Engineering Manufacture, 216(12), 2002, pg. 1621-1634.
5. N. Hopkinson, P. Dickens, Rapid prototyping for direct manufacture, *Rapid prototyping J.*; 7,4; 2001, pg. 197.
6. Wohlers, T. *Past, present and future of rapid prototyping*. International Journal of Product Development, 1(2), 2004, pg. 147-154.
7. 3D Systems *3D Systems: Customer success*. Available from www.3dstystems.com [Accessed 16/4/05]
8. Carter, P. W. *Advances in rapid prototyping and rapid manufacturing*. Paper presented at the Electrical Insulation Conference and Electrical Manufacturing and Coil Winding Conference (EIC/EMCW Exposition 2001), Oct 16-18 2001, Cincinnati, OH.
9. Levy, G. N., Schindel, R., & Kruth, J. P. *Rapid manufacturing and rapid tooling with layer manufacturing (LM) technologies, state of the art and future perspectives*. *CIRP Annals - Manufacturing Technology*, 52(2), 2003, pg. 589-609.
10. N. Hopkinson, P. Dickens, Analysis of rapid manufacturing-using layer manufacturing processes for production, *Proc. Instn. Engrs Vol. 217 part C*, 2003, pg. 31-40.
11. Materialise, *Selective laser sintering*. Available from www.materialise.com/prototypingsolutions/laser_ENG.html, [Accessed 15/12/04].
12. Nelson, J. C., Xue, S., Barlow, J. W., Beaman, J. J., Marcus, H. L., & Bourell, D. L., "Model of the selective laser sintering of bisphenol-A polycarbonate", *Industrial & Engineering Chemistry Research*, 32(10), (1993), 2305-2317.
13. Caulfield, B., McHugh, P. E., & Lohfeld, S. *Dependence of mechanical properties of polyamide components on build parameters in the SLS process*. *Journal of Materials Processing Technology*, 182(1-3), 2007, pg. 477-488.
14. Zhang, J., Xu, Z.-F., Zheng, H.-Z., & Huang, Y.-H. *Preparation of polymer/Aluminium Oxide nano-composites by selective laser sintering*. *Cailiao Gongcheng/Journal of Materials Engineering*(5), 2004, pg. 36-39.
15. Wang, Y., Shi, Y., & Huang, S. *Selective laser sintering of polyamide-rectorite composite*. Proceedings of the Institution of Mechanical Engineers, Part L: Journal of Materials: Design and Applications, 219(1), 2005, pg. 11-16.
16. J.H.Koo, S.Lao, W.Ho, K.Nguen, J.Cheng, L.Pilato, G.Wissler, M.Ervin, Polyamide nanocomposite for SLS, in proc. 2006 SFF symposium.
17. Chung, H., & Das, S. *Processing and properties of glass bead particulate-filled functionally graded Nylon-11 composites produced by selective laser sintering*. *Materials Science and Engineering A*, 437(2), 2006, pg. 226-234.
18. Vollath, D., & Szabo, D. V. Synthesis and Properties of Nanocomposites. *Advanced Engineering Materials*, 6(3), 2004, pg. 117-127.
19. NPL, Nano-Composites Long-term Mechanical Properties. [Accessed 15/12/04]. Available from World Wide Web: http://nanomaterials.npl.co.uk/composites/nano_comp2.html
20. AMR, *Material data sheet for yttrium stabilized zirconia (YSZ)*. AMR Technologies Inc. 2006
21. Elementies, *Material data sheet for Benton 166*. Elementies Specialist, 2004.
22. Goodfellow, *Material datasheet for PA6*, 2006.
23. ASTM D638-03 Standard Test Method for Tensile Properties of Plastics. ASTM International
24. C. Hauser, *Selective laser sintering of stainless steel powder*, PhD Thesis, 2003, University of Leeds.
25. Fong, H., Chun, I., & Reneker, D. H. *Beaded nanofibers formed during electrospinning*. *Polymer*, 40(16), 1999, pg. 585-4592.
26. A.V. Sessa, T. Inoue, K.Yonetake, K. Koyama *Thermal behaviour of poly (acryloyloxybenzoic acid)/nylon 6 blends*, *Polymer*, v 42, n 24, 2001, 985-962.